

Mitigation of Micro and Macro Bends for Improved Bandwidth in Fiber Optics Communication

P. Elechi^{1*}, S. Orike², P. C. Anumbe³

¹Senior Lecturer, Department of Electrical/Electronic Engineering, Rivers State University, Port Harcourt, Nigeria

²Senior Lecturer, Department of Computer Engineering, Rivers State University, Port Harcourt, Nigeria

³PG Student, Department of Electrical/Electronic Engineering, Rivers State University, Port Harcourt, Nigeria

*Corresponding Author: elechi.promise@ust.edu.ng

ABSTRACT

The importance of bending loss of polarization maintaining optical fiber can never be over emphasized in optical systems and active organised communication. To attain a polarized state of a wave that is confined to a certain plane moving at a direction of propagation, an internal stress introduced by an elliptic cladding generates a polarization and propagation characteristics that determine the refractive index that is brought about by stress. To simulate and obtain the bending loss of the PM fiber, two different models were adopted. Model 1 involved carrying out a simulation process to determine the losses caused by bending within the PM fiber, this model did not consider the photo-elastic effect of the bending. Model 2 handled the possible change of refractive index occasioned by bending stress. Interestingly, the results obtained from the experiment was in corresponding pattern with what was obtained in Model 1 and Model 2 of the waveguide. In order to derive a standard variation that occur between two different cases of bending with distinct far reaching orientation, then the results obtained from the simulation and experiment only disagreed by a factor of 2 or 3 while considering small radii of curvature. 0.76 was obtained from the experiment and 0.28 was obtained from the simulation, all from a radius of 3.5mm. From observation, it became obvious that repeated order of bending loss of the PM fiber confirmed that the fashion through which bending losses occur within the PM fiber were minimal when the polarization is pointed along the major axis within the elliptical cladding and in the same direction with the plain of curvature. The bending loss obtained from the polarization of the propagating wave and radius of curvature are not disregarded and must be on the same direction of polarization.

Keywords-- Bending, communications, fiber, networks, wave

INTRODUCTION

Background of the Study

Optical fiber in optical networks today convey hundreds of terabits per second to destinations all over the world, carried by multi-coloured laser signals [1]. This is a dividend of several researches done over the years to meet up with the desire to maximize bandwidth, reduce attenuation and counter the electromagnetic interference from surrounding environment of the network. A typical optical network system consists of the light source which often is the laser wave, the waveguide, which in this case is the optical fibre and a repeater to amplify the signals in event of signal losses before getting to the destination and then the receiver at the other end of the network. One of the key elements in the fiber optics revolution has been the dramatic improvement in the transmission characteristics of optical fibers [2]. This drastic improvement has endeared the optical fibre as one of the most sorted waveguides in the telecommunication industries. Part of the optic fibre is the core, made up of glass. This core serves as a channel through which the light travels. The presence of the core cladding; an outer cover that serves as insulation that reflects back the light to curtail radiative loss of signal. There is also the buffer coat that ensure the protection of the cable from moisture. A number of factors affects the performance of the optical fibre some of which includes Scattering, Dispersion, Micro bending loss etc. These fiber attributes define the spans between regenerators and the signal transmission rates [3].

It is widely understood by optical fiber users that severely bending a live optical fiber will incur an optical power loss, and the received signal power will be reduced. One way to observe the effect of bending losses is to use a Visual Fault Locator (VFL) where the visible red-light glow seen at the point of bend indicates light escaping from the fibre core, passing through the cladding and fibre coatings before escaping into the environment [4]. A second way to observe bending losses is to use an OTDR in real time mode where a

severe induced bend causes a noticeable drop in the backscattered power level beyond the point of bending.

Micro bending (bends too small to be seen with the naked eye) occur when pressure is applied to the surface of an optical fibre [5]. The pressure applied to the surface results in deformation of the fibre core at the core-cladding interface. Micro bending losses occur when surface pressure causes numerous tiny contact point indentations on the fiber surface even though the fiber itself may be laid out straight. The light intensity will suffer losses when light signal transfers through the optical fibre due to the presence of curvature in the fiber path that is assumed to be straight along the light propagation line [6].

Review of Related Work

Investigation for improved bend loss formula was verified in Optical Fiber using Simulation and Experiment by [7]. The work presented an improved curvature loss formula for optical waveguides, which was used to accurately predict the bend loss of both single-mode and multimode fibers. The formula expands upon a previous formula derived by Marcuse, greatly improving its accuracy for the case of multimode fiber. Also presented are the results of bent fiber simulations using the beam propagation method (BPM), and experimental measurements of bend loss. Agreement among simulation, formula and measurement support the validity of both theoretical methods. BPM simulations showed that the lowest order modes of the bent fiber were reduced to their linearly polarized constituents prior to the onset of significant bend loss. This implies that certain LP mode orientations should propagate with much lower loss than previously expected, and should impact the mode stripping ability of bent large mode area fibers, as employed in fiber lasers and amplifiers.

Researchers investigated the optimization of macro bending loss in small and large mode area photonic crystal fibers, the use of low bend loss optical fibers in fiber-to-the-home (FTTH) networks becomes unavoidable to improve the optical networks performance [8]. One of the candidates is photonic crystal fibers (PCFs) for their low bend loss properties. This paper presents procedures for optimization of the bend loss of PCFs with small and large mode areas by using solvers Software (Rsoft and Optifiber). The optimizations are performed with respect to bend radius, core radius, photonic crystal pitch and the ratio of air-filling factor. The lowest bend loss of 1 dB/cm was obtained at bend radius of 56 mm and core diameter of 22 micrometer.

Investigated micro bending effect in single mode optical fiber investigation and novel applications, from his analysis, the operating wavelength was shown to be tuneable by changing the spatial period of the deformation, thereby deriving an extinction ratio of 25dB with an attenuation of 1.3dB, at an operating wavelength of 1177nm [9].

Researched on the wavelength- dependent bend loss in a step-index multimode fiber optic micro-bend displacement for optical fiber (100 μ m), bend radii ranging between 2.0 and 4.5 mm using six excitation wavelengths, namely, 337.1, 470, 590, 632.8, 750 and 810nm [10]. A novel micro bend fiber – optic acoustic sensor has been studied, both analytically and experimentally, using a simple mechanical sensor, insensitive to acceleration, and achieves shape flexible by utilizing fairly long fiber lengths for the sensing element [11].

Analysed G.652.D and G.657.A2 using teeth connector experimental setup to experimentally scrutinize the attenuation loss that occur due to displacement of cladding layer within the optical fiber due to the stress generated by the current flow in conductor [12]. The step size was taken as 0.01mm to create the micro-bend in the optical fiber and analyse the number of micro bends the optical fibre can handle for the attenuation loss to 0.15dB/km.

MATERIALS AND METHOD

Materials

The following materials were employed in this work

3M – FS –PM-6621 with Dimensions

[Wavelength :1300nm, Mode field diameter: 9.0 \pm 0.5 μ m, Core diameter: 8.2 \pm 0.5 μ m (This is the value of Mode field diameter, 10% less), Diameter of the fiber: 125 μ m]

The Measurements for the 2nd Mode

[Cut-off wavelength: < 1270nm, Numerical aperture: 0.13, n_2 which represents the Refractive index of the inner cladding: 1.453, n_1 , Which represents the Refractive index of the core :1.459, The change in the refractive index between the inner cladding and the core cladding, Δn : 0.006 i. e $\Delta n = 0.41\%$, The birefringence between x and y with respect to the difference in refractive index, δn : 4.3×10^{-5} .

The Experimental Framework

1.45 μ m laser diode, polarizer, A half – wave plate, A lens, two fibre holders, two orbiting adjusters, A bending device, A photodiode, An oscilloscope.

Method

There is a high tendency of curved waveguide emitting radiation at incidence of light,

without recourse to stress and birefringence in the fibre. To be able to carry out a simulation to arrive at a conclusive result, three models of the bent PM fibre was considered in relation to curved planar waveguides.

Model 1: Refractive index profile ascribed to a straight waveguide is the focus of this model. Various radii of curvature were the basis of calculation of the Bending loss

Model 2: A critical study of the refractive index change was the basis of this model.

Model 3: The photo elastic effect brought about by bending stress in connection to stress induced by ellipsoidal cladding directed along the major axis is

the bedrock upon which this model was designed. Additionally, a further consideration of the several linear profiles that yield eccentric waveguide to yield bending loss directly is also part of the design of the model. Adding the refractive index variation in the calculation is one of the highlights of this method.

With the use of a 3M Polarization Fibre, the experiment as shown in Fig. 1 focused on showing the clear-cut variations between bending losses of fibre when bent at distinct axis. It is expected that the result obtained from the experiment should be in the same range with what is obtained from the simulation result.

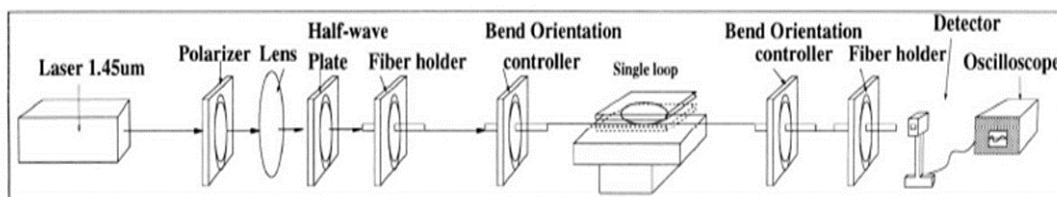


Figure 1: Experimental arrangement.

Fig. 2 is the view under a microscope showing the various axis, i.e., the major axis and the minor axis and the varying bending orientations.

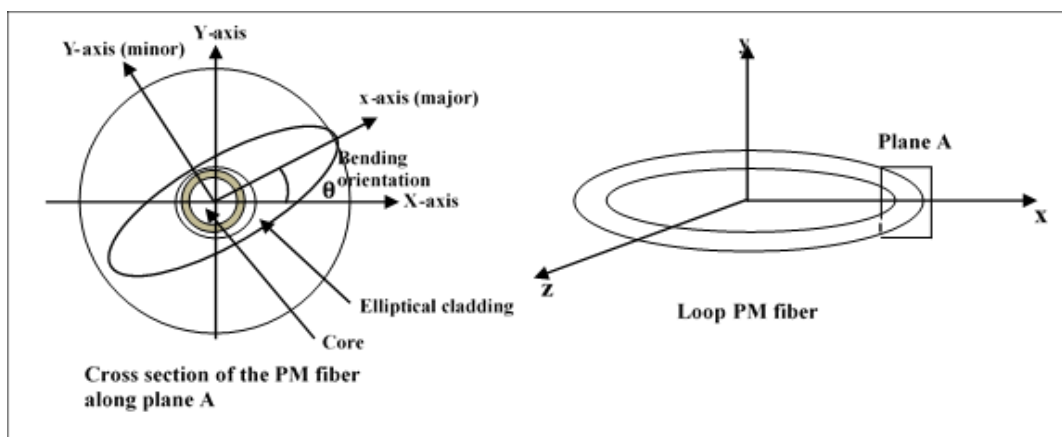


Figure 2: Random view of PM fibre along X, Y plane.

Adjusting the bending orientations entails interfacing two rotational clencher with the loop sandwiched in between. Because the orientations are measured in degrees, the both clencher are

scaled in degrees to enable easy reading of orientation in degrees [13]. This arrangement entails the arrangement of two translucent sheets with a dividing space. This is shown in Fig. 3.

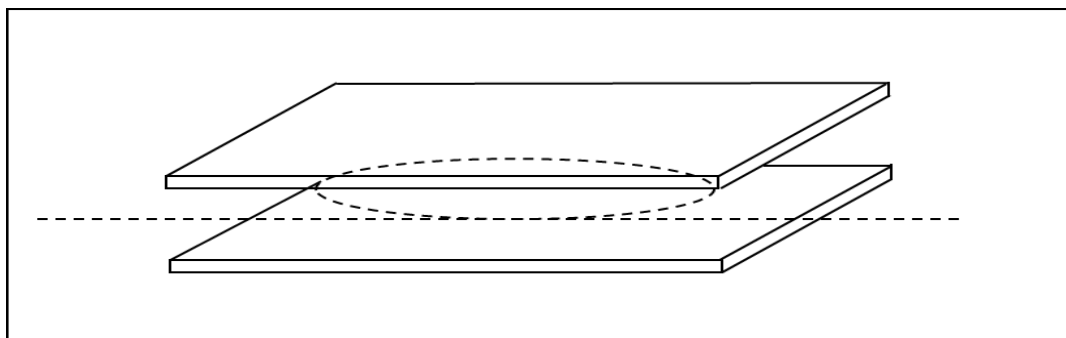


Figure 3: Bending device.

One peculiarity of the setup above is the ability to form a circular loop out of a fibre and yet not add an extra stress on it. The rotational controller on and before the bending device and the bending device itself is useful to estimate the bending loss of the loop while tilted along different orientations [14].

Procedures

Fine-tuning the x, y, z coordinates of the lens will enable the linearly polarized light to be on its course into the PM fibre. The major axis as arranged in the PM fibre is expected to compliment with the polarization direction. To attain that, the source polarization is adjusted through a continuously swivel half-wave sheet until the output of the maximum extinction ratio is reached. The value obtained for the straight polarization maintaining fibre is documented for reference P(0). The small loop formed of the PM fibre with the aid of the bending device is of radius 6mm. The

oscilloscope aided in retrieving the power of output. Between the degrees of 0 to 180 orientations. The controller is rotated for each desired orientation. For every 20 degree, the power of output is captured and documented. Subsequent experiments entailed changing the curvature of the radius R_c from 6mm to 3mm by 0.5mm. This is continuously done until the fibre elastic limit is exceeded and the strain becomes irreversible.

The bending loss in the experiment was computed using equation (1) [14].

$$\frac{10}{L} \log(p_{out}/p_{in}) \quad (1)$$

The relationship between the ending loss and attenuation factor γ of the curved fibre was computed using equation (2) [15].

$$\frac{10}{L} \log(p_{out}/p_{in}) = 10 \log(e)\gamma = 4.343\gamma \quad (2)$$

This implies that the bending loss increased at a rapid rate as the radius of curvature R_c decreased. A linear function R_c was obtained when the logarithm of bending loss was taken.

RESULTS AND DISCUSSION

Results

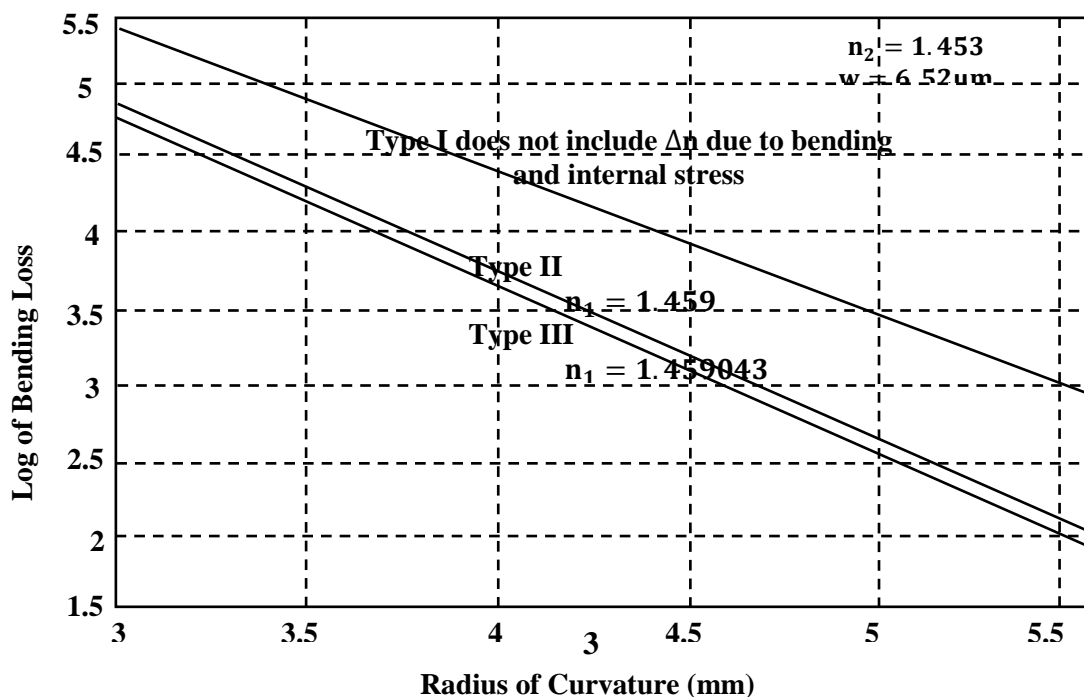


Figure 4: Bending loss of fibre versus several refractive index profile.

As noticed in model 1, the bending loss in the optical fibre increased rapidly with a corresponding decrease in the bending radius of the waveguide. The values of the logarithm of bending matched against the various refractive index profiles as illustrated in Fig. 4. As can be deduced from Fig. 4, the three models are duly represented.

In the first model, the bending loss of the waveguide is captured without a consideration of a change in refractive index occasioned by the effect of internal and bending stress due to elliptical cladding. From observation, it showed that in this scenario, a higher bending loss was recorded against what is obtained in the rest of the other two

scenarios. It is typical to simulate loss caused by bending using this model at instances when the plane of curvature and the polarizing wave direction are at a perpendicular position. The resemblance between the first type of waveguide

and the refractive index profile directed along the polarization direction is basically because along this direction, the impact of stress caused by bending is not felt as illustrated in Fig. 5.

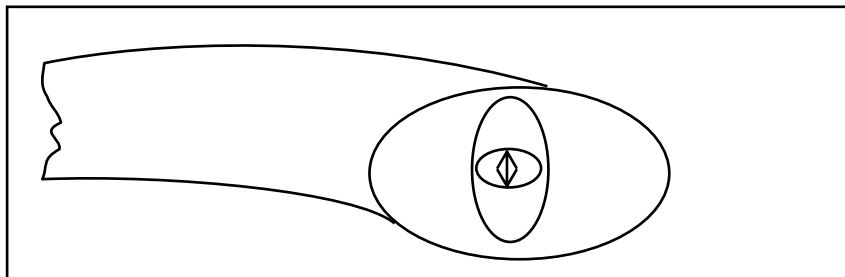


Figure 5: Polarization direction of model 1 and the corresponding orientation of the elliptical cladding.

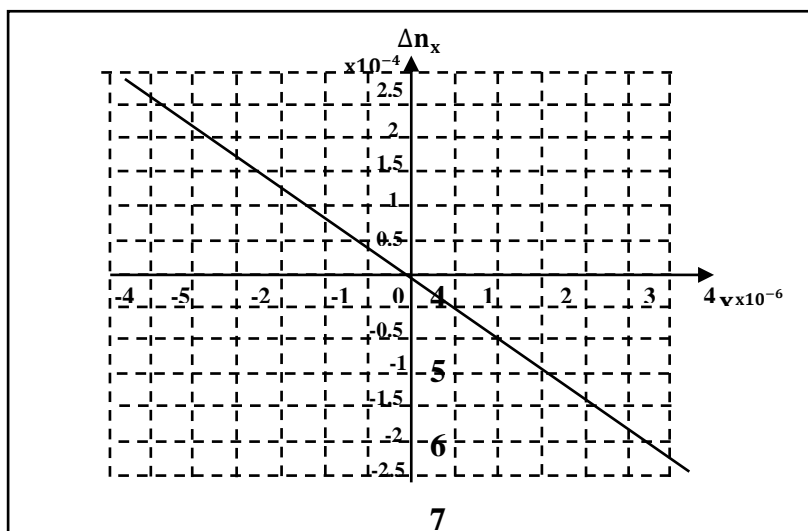


Figure 6: Refractive index variation along the y direction induced by bend stress.

Fig. 6 confirms that along the y direction, effective index cannot be altered as a result of stress caused by bend. That is, at the origin, Δn_y is nearest to zero (i.e., $x=0$). Fig. 7, illustrates the polarization direction and elliptic cladding orientation associated with the wave. The loss common with bend in the PM fibre is associated with various factors which include; the direction of polarization and the orientation of bend within the

fibre. Also, captured is the radius of curvature. These have been confirmed from the result of the experiment conducted to this regard. It is discovered that when wave polarization is directed along the main axis, as well as the orientation of bend at zero, the signal loss is drastically reduced (Fig. 8). It is very glaring as shown in Fig. 9 that more losses associated with bend is at its peak when orientation of the fibre is at 90 degrees.

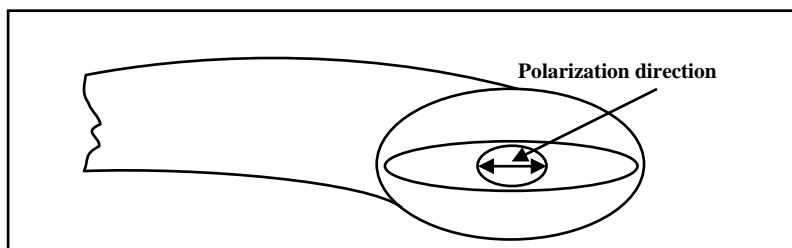


Figure 7: Lower bend loss: Orientation of bend and polarization direction.

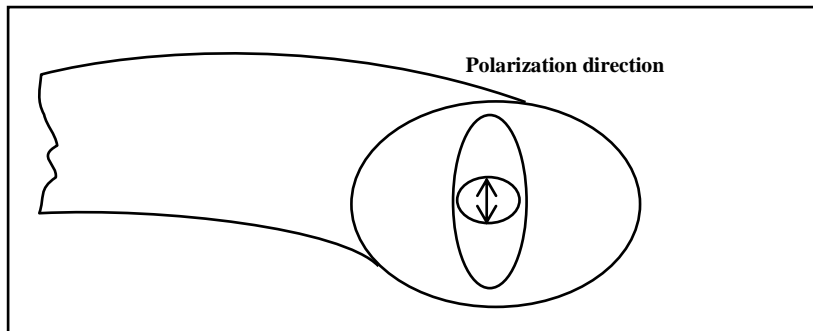


Figure 8: Higher bend loss: Orientation of bend and polarization direction.

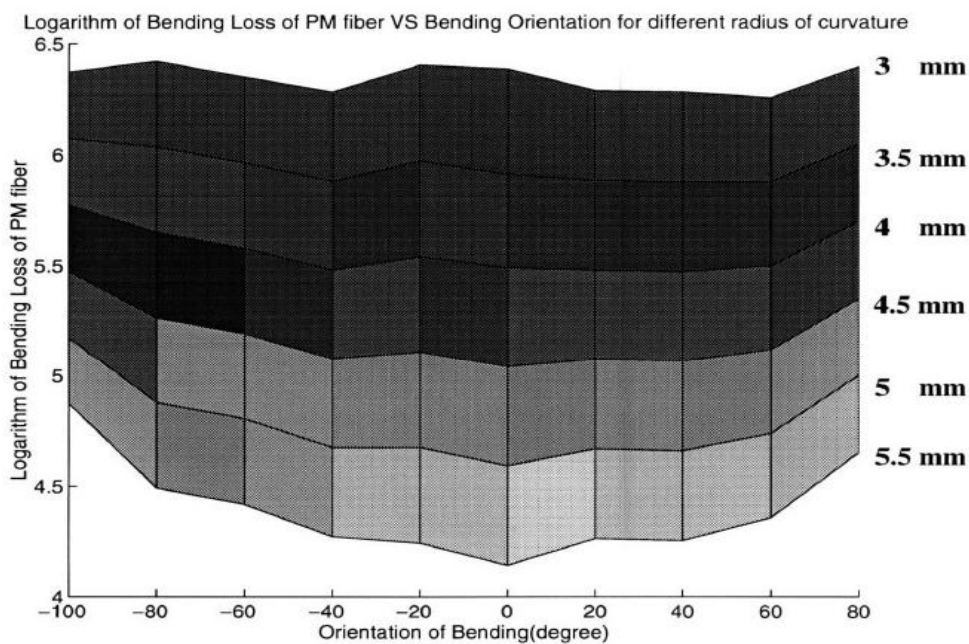


Figure 9: Logarithm: Radius of curvature, bend loss versus orientation of bend.

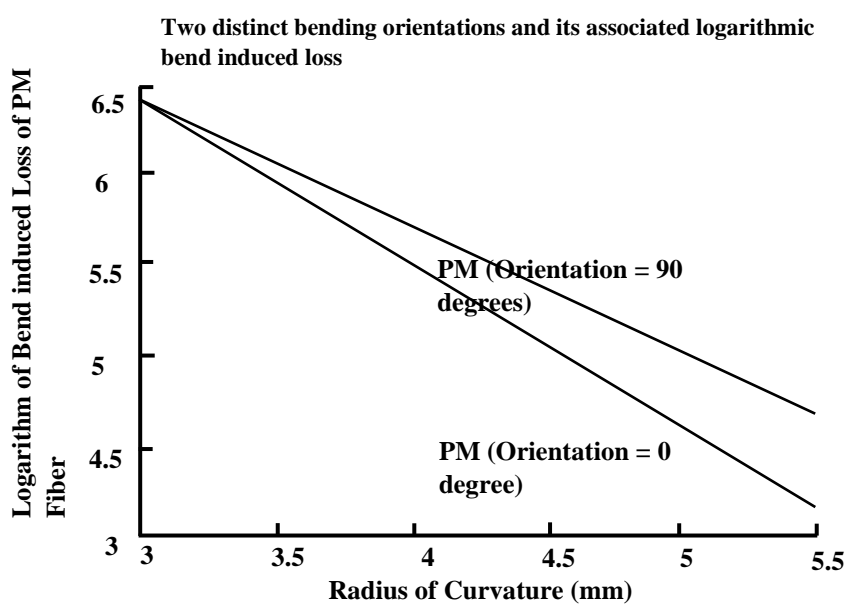


Figure 10: Experimental data: Two distinct bending orientations at 90 and 0 degrees and its associated logarithmic bend induced loss.

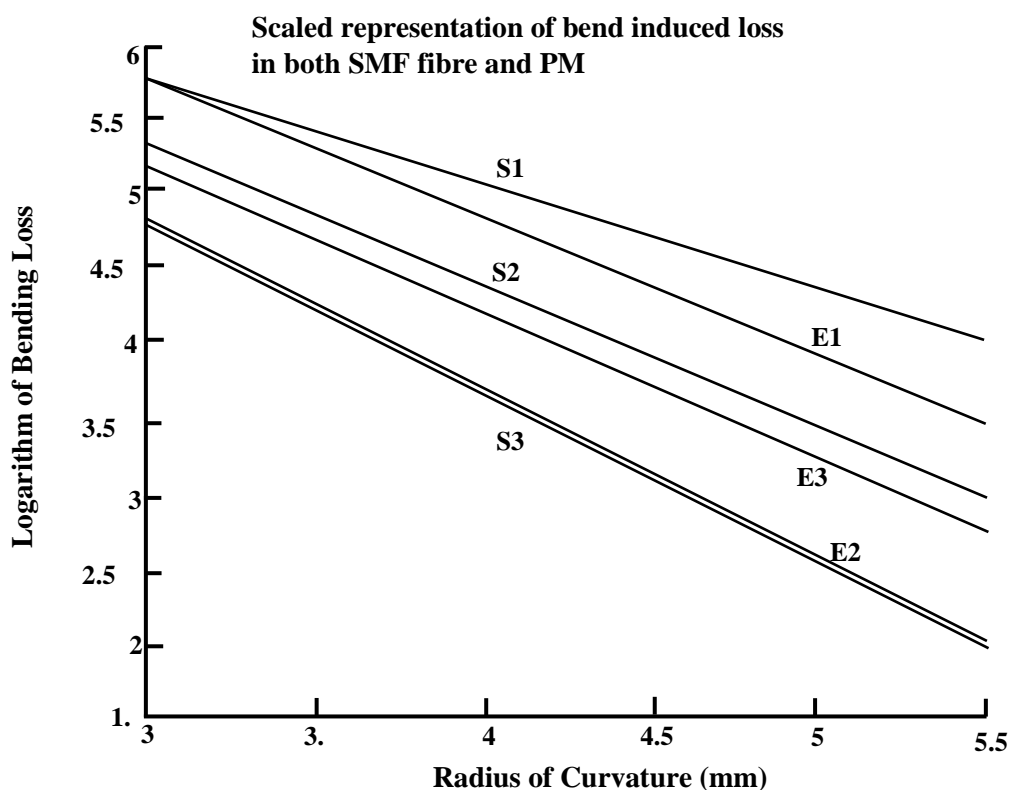


Figure 11: Representation of merged results of experimental and simulated bend induced loss.

A similar result of bending loss obtained in type 1 as depicted in Fig. 4 is also obtained in PM fibre bended within a 90 degrees orientation. This can be seen in Fig. 11. In Fig. 10, along the y – axis, the bend induced stress does not result to any alteration. This unaltered refractive index also lies parallel to the polarization direction along the propagation wave.

There is a conformance between the recorded bend loss in the type III waveguide and that of the lower curve shown in Fig. 10. To carry out a complete analysis of the results from the simulation and that from the experiment, the separate graphs representing each scenario and the result is merged using a common logarithmic scale.

Table 1: Type of fiber for experimental and simulation and their orientation.

S/N	Symbol	Type of Result	Orientation in degree	Type of Fibre
1.	E1	Experiment	90	PM Mode Fibre
2.	S1	Simulation	90	PM Mode fibre
3.	E2	Experiment		Single Mode fibre
4.	S2	Simulation		Single Mode fibre
5.	E3	Experiment	0	PM fibre
6.	S3	Simulation	0	PM fibre

The representation above showcases the bending loss in the experiment on the PM fibre depicted by E1, E2, E3, S1, S2, and S3 when the plane of curve and the direction of polarization are at perpendicular (Table 1). This is shown in Fig. 11. E2 and S2 on the other hand signifies the single mode fibre with non – PM attributes. On the contrary, at polarization along a direction parallel to the plane of curvature, the bend induced loss is denoted as E3 and S3 as can be seen portrayed in Fig. 11. It can be gathered from the duo results of

the experiment and the simulation that the variation between the two obtained results is only differed by a factor of 3. The fact that the two results are in a similar order of magnitude validates the comparative outcome of the two approaches. 5.6B/cm could be a specific value of bending loss for radius of curvature of 3mm of a PM fibre. Between E1 and E2, S1 and S3, the changes in bending loss are normalized as portrayed in Table 2.

Table 2: Normalized PM fibre bending differentials obtained on polarization direction when alignment with curvature plane, i.e., 0-degree orientation and while at perpendicular to curvature plane, i.e., 90-degree orientation.

Radius of Curvature(mm)	Simulation Outcome	Experimental Outcome
03.0	0.71	0.18
03.5	0.77	0.29
04.0	0.82	0.41
04.5	0.86	0.54
05.0	0.89	0.64
05.5	0.91	0.72

Plainly looking at the result, we can posit that at extreme cases of bending, the bending loss differences obtained from the experiment which in this case has been normalized are in factor of 2 or 3 for the smallest radii of curvature. We can,

therefore, rightly see that a high probability of obtaining matching results for bending loss from the experiment and simulation at radii of curvature that equals 4.5mm is very much feasible (Fig. 12).

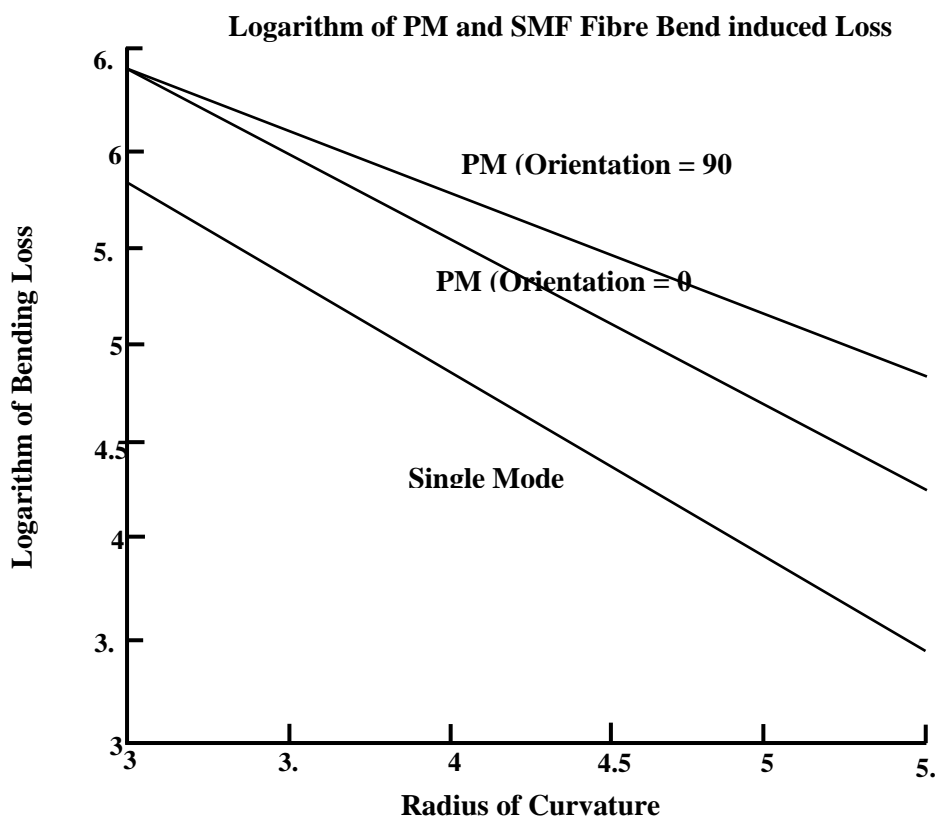


Figure 12: Bending loss of PM fibre and SMF with respect to radius of curvature.

CONCLUSION

Mitigation of Optical bending loss in Polarization Maintaining Optical fibre and Single Mode fibres are very paramount for an adequate deployment of efficient optical telecommunication needs in optical sensing systems and telecommunication systems as a whole. Several factors such as the bending Orientation of a fibre, Curvature radius and direction of polarization

affect the bend loss common in PM fibre. The elliptic cladding is an important aspect of the PM fibre in that it builds up the internal stress which in turn enlarges the refractive index variation between the cladding and the core. This pulls the power to the core; consequently, minimal bend loss is recorded. Tilted step profile is arrived at when variation in refractive index is experienced, influenced by stress originating from fibre bend. The uniform step waveguide gets to be more

radiative than it would be in the effective index profile. This experimental outcome authenticates this peculiarity in bending loss. There is a substantial decrease in bending loss at the instance a polarized wave of the waveguide is directed as that of the elliptical cladding along the major axis. On the other hand, there is an upsurge of bend loss when the polarized wave in a PM wave guide is directed in a direction perpendicular to the curvature plane. At an orientation, $\theta = 90$ degrees and $\theta = 0$ degrees, the level of bending loss is determined when variation of the two distant orientations at varying range of radius in the order of 10^3 to 10^6 dB/km is employed. There is an upsurge in this variation when the curvature radius declines. The photoelastic induced refractive index inclines when there is a decline in in the bending radius. This is making reference to the fact that along the $x - axis$ and the $z - axis$ the associated stress are functions of $\frac{1}{R^2}$ and $\frac{1}{R}$ respectively. The influence of the minimal radius of curvature caused by stress is the major cause proponent of bending loss. It is, therefore, ascertained that a decline in the bending radius is a resultant effect of an increase in the bending loss difference. SMF-28 Bending fibre loss can, therefore, be concluded as verified from the experiment to be relatively lower than the bending loss of the 3M-FS-PM-6621 fibres. This kind of validates the earlier projected pattern. As can be seen in Fig. 4, type 1 curve fibre, shows a direction of polarizing wave along the waveguide perpendicularly aligned along the plane of curvature in a PM fibre, The SMF bending loss declines lower than the bend loss of a PM fibre. We can attribute this to the inability of the photo elastic effect resulting from bending to vary the effective index profile on the $y - axis$ of the PM fibre. In the case of the SMF, there is an alteration cause by the bend induced photo elastic effect on the refractive index profile. This aids in confining to the core the mode power. We can now round up by saying that attenuation and radiative loss in the core and PM fibre respectively is drastically reduced by the induced bend stress, adequate bended orientation, direction of polarization and the radius of curvature.

RECOMMENDATIONS

Against our earlier projection, the experimental result does not coincide with the desired predictions. Experimental results showed a pattern that agrees that the bending loss of SMF is less than that of the PM fibre. Whereas, it is typical that when the direction in a PM fibre is aligned along the major axis of the elliptical cladding and is parallel with respect to the curvature plane, the loss in the PM fibre as a result of bend is less than loss

caused by bend observed in SMF. In light of this, we recommend that further studies and deployment of more models could be undertaken to ascertain the veracity and level of deviation from the earlier stated projection.

REFERENCES

1. M. Galili, F. Da Ros, M. Pawel, G. Rademacher, et al., "Characterization and optical compensation of LP01 and LP11 intramodal nonlinearity in few-mode fibers", *Opt. Soci. of America*, Volume 6, Issue 6, pp. 234-239, DOI: 10.1364/OFC.2020.Th1H.4.
2. A. Ghatek, K. Thyagarajan, "Introduction to fiber optic", Cambridge University Press, London.
3. P. Elechi, S. Orike, D.A. Echendu (2020), "Simulated bandwidth improvement of hexagonal circular photonic crystal fiber using hybrid cladding", *J. of VLSI Design and Sig. Proces.*, Volume 6, Issue 3, pp. 10-24
4. L. Faustini, G. Martini (1997), "Bend loss in single-mode fibers", *IEEE J. of Light Wave Tech. Lett.*, Volume 15, Issue 3, pp. 671-679, DOI: 10.1109/50.566689.
5. N. Unger, O. Gough (2008), "Life cycle considerations about optic fibre cable and copper cable systems", *J. of Clean. Prod.*, Volume 16, Issue 14, pp.1517-1525, DOI: 10.1016/j.jclepro.2007.08.016.
6. K. Roberts, M. O'sullivan, W. Kuang-Tsan, S. Han, A. Awadalla, D. J. Krause, C. Laperle (2009), "Performance of dual-polarization QPSK for optical transport systems", *J. of Lightwave Tech.*, Volume 27, Issue 16, pp. 3546-3559.
7. M. A. Mahdi, Y. M. Kamil (2018), "Sensors and actuators", *Sci. Dir.*, Volume 257, Issue 6, pp 820-828.
8. T. Ross, K. Schermer, H. James (2007), "Improved bend loss formula verified for optical fiber by simulation and experiment", *IEEE J. of Quant. Electron.*, Volume 42, Issue 10, pp. 889-909, DOI: 10.1109/JQE.2007.903364.
9. E. S. Faramarz (2015), "Impact of dynamic pressure and thermal loading on refractive index and microbending loss in two-layer optical fibers", *Internat. J. of Opt. and App.*, Volume 5, Issue 5, pp. 168-179, DOI: 10.5923/j.optics.20150505.05.
10. V. Arya, A. Kent, A. Wang, O. Richard (1994), "Microbending losses in single mode optical fiber: theoretical and experimental investigation", *J. of Lightwave Tech.*, Volume 13, Issue 10, pp. 1988-2002, DOI: 10.1109/50.469736.

11. S. Addanki, P. Yupapin (2018), "Review of optical fibers-introduction and applications in fiber lasers", *J. of Res. in Phy.*, Volume 10, Issue 8, pp. 743-750, DOI: 10.1016/j.rinp.2018.07.028.
12. N. Lagakos, W. J. Trott, T. R. Hickman, H. C. James, J. A. Bucaro (1982), "Microbend fiber-optic sensor as extended hydrophone", *IEEE J. of Quant. Electron.*, Volume 18, Issue 10, DOI: 10.1109/JQE.1982.1071433.
13. A. Ashfaq, M. Awais, S. A. Ali, W. Ejaz, A. Anpalagan (2019), "Resource management in multicloud iot radio access network", *IEEE Int. of Things J.*, Volume 6, Issue 2, pp. 3014-3023, DOI: 10.1109/JIOT.2018.2878511.
14. P. Elechi, S. Orike, W. Mina-Eeba (2018), "Simulated sensitivity improvement of optical receiver in fiber optic network", *Adv. in Appl. Sci.*, Volume 3, Issue 4, pp. 43-51, DOI: 10.11648/j.aas.20180304.11.
15. P. Elechi, S. Orike, W. Minah-Eeba, C. E. Ikpo (2018), "Sensitivity analysis of avalanche photodiode and PIN diode detectors in optical receivers", *J. of Eng. Stud. and Res.*, Volume 24, Issue 4, pp. 1-11, DOI: 10.29081/jesr.v24i4.303.